Priority Report

Cancer Research

Evaluating Patient-Derived Colorectal Cancer Xenografts as Preclinical Models by Comparison with Patient Clinical Data

Manoel Nunes[1,2], Patricia Vrignaud[1,2], Sophie Vacher[3], Sophie Richon[4], Astrid Lièvre[5,6], Wulfran Cacheux[5], Louis-Bastien Weiswald[4], Gerald Massonnet[7], Sophie Chateau-Joubert[8], André Nicolas[9], Colette Dib[1,2], Weidong Zhang[1,2], James Watters[1,2], Donald Bergstrom[1,2], Sergio Roman-Roman[7], Ivan Bièche[3,4], and Virginie Dangles-Marie[4,7]

Abstract

Development of targeted therapeutics required translationally relevant preclinical models with well-characterized cancer genome alterations. Here, by studying 52 colorectal patient-derived tumor xenografts (PDX), we examined key molecular alterations of the IGF2–PI3K and ERBB–RAS pathways and response to cetuximab. PDX molecular data were compared with that published for patient colorectal tumors in The Cancer Genome Atlas. We demonstrated a significant pattern of mutual exclusivity of genomic abnormalities in the IGF2–PI3K and ERBB–RAS pathways. The genomic anomaly frequencies observed in microsatellite stable PDX reproduce those detected in nonhypermutated patient tumors. We found frequent *IGF2* upregulation (16%), which was mutually exclusive with *IRS2*, *PIK3CA*, *PTEN*, and *INPP4B* alterations, supporting *IGF2* as a potential drug target. In addition to maintaining the genomic and histologic diversity, correct preclinical models need to reproduce drug response observed in patients. Responses of PDXs to cetuximab recapitulate also clinical data in patients, with partial or complete response in 15% (8 of 52) of PDXs and response strictly restricted to *KRAS* wild-type models. The response rate reaches 53% (8 of 15) when *KRAS*, *BRAF*, and *NRAS* mutations are concomitantly excluded, proving a functional cross-validation of predictive biomarkers obtained retrospectively in patients. Collectively, these results show that, because of their clinical relevance, colorectal PDXs are appropriate tools to identify both new targets, like IGF2, and predictive biomarkers of response/resistance to targeted therapies. *Cancer Res; 75(8); 1560–6. ©2015 AACR.*

Introduction

Colorectal cancer remains a major cause of mortality worldwide and colorectal cancer patient death is generally attributable to metastasis development. Comprehensive molecular characterization of colorectal cancer has identified key gene and pathway alterations important for initiation and progression of colorectal cancer, including alterations in the PI3K and ERBB–RAS pathways (1, 2). Some genetic anomalies have been also shown to predict response to specific therapies, such as activating mutations in *KRAS*, which predict resistance to anti-EGFR monoclonal antibodies (MAb; ref. 3). For efficient development of new therapies and companion biomarkers, preclinical models mimicking the molecular epidemiology and drug sensitivity of human tumors are needed.

In colorectal cancer, tumor-specific patient-derived xenograft (PDX) models have shown to retain the intratumoral clonal heterogeneity, chromosomal instability, and histology of the parent tumor through passages in mice (4–7). To extend these observations, we investigated here a collection of 52 colorectal PDXs (6), composed of 48 microsatellite stability (MSS) and four microsatellite instability (MSI) tumors, for the presence and prevalence of molecular features reported in large colorectal cancer patient cohorts (1, 2, 8). In particular, we studied key alterations in IGF2–PI3K and ERBB–RAS pathways and the role of these alterations in predicting response to cetuximab.

Materials and Methods

Patient-derived tumor xenografts

Tumor xenografts were established directly from patient tumors (6) and were routinely passaged by subcutaneous

[1]Translational and Experimental Medicine, Sanofi Oncology, Sanofi, Vitry-sur-Seine, France. [2]Translational and Experimental Medicine, Sanofi Oncology, Sanofi, Cambridge, Massachusetts. [3]Service de Génétique, Hôpital Institut Curie, Paris, France. [4]IFR71, Faculté de Sciences Biologiques et Pharmaceutiques, Université Paris Descartes, Sorbonne Paris Cité, Paris, France. [5]Département d'Oncologie médicale, Hôpital Institut Curie, Paris, France. [6]Université de Versailles Saint-Quentin en Yvelines, Faculté des Sciences Biologiques, Versailles, France. [7]Recherche Translationnelle, Centre de Recherche, Institut Curie, Paris, France. [8]France Université Paris-Est, Ecole Nationale Vétérinaire d'Alfort, Unité d'Anatomie Pathologique, Maisons-Alfort, France. [9]Département de Pathologie, Hôpital Institut Curie, Paris, France.

Note: Supplementary data for this article are available at Cancer Research Online (http://cancerres.aacrjournals.org/).

Current address for P. Vrignaud: Direction de la Recherche, Institut Gustave Roussy, 114, Villejuif, France; current address for Sophie Richon, UMR144, Centre de Recherche, Institut Curie, Paris, France; current address for L.-B. Weiswald, Division of Gastroenterology, Department of Medicine, University of British Columbia, Vancouver, British Columbia, Canada.

Corresponding Author: Virginie Dangles-Marie, Research Center, Institut Curie, 12 rue Lhomond, F-75005 Paris, France. Phone: 33-156246321; Fax: 33-156246330; E-mail: virginie.dangles-marie@curie.fr

doi: 10.1158/0008-5472.CAN-14-1590

engraftment in immunodeficient CB17-SCID mice (Charles River Laboratories). Xenografts, passage P6-P9, were harvested from 3 mice for each model, when they reached around 150 to 300 mm^3 in size for RNA and DNA extraction. For *in vivo* pharmacological studies, cetuximab (Imclone) was given at 12.5 mg/kg/adm, (Q3D×2) ×2 i.p.), mice bearing 100 to 200 mm^3 tumors at start of therapy ($n = 8–10$ per group) as already described (6). All experimental procedures were approved by Sanofi Laboratory Animal Care and Use committee.

MSI status

MSI testing was performed according to the National Cancer Institute guidelines using a five-microsatellite consensus panel (6).

DNA sequencing

Next-generation sequencing and mutation calling were performed at Beijing Genomics Institute (BGI). Library preparation was performed using exome capture Agilent SureSelect All Exon 50M. Libraries were sequenced using the Illumina HiSeq platform. Quality single-nucleotide polymorphism (SNP) calling criteria have been applied: SNP quality is equal or greater than 20; the minimum sequencing depth is 4× and the mean is 100×, with 99% of coverage target region. To evaluate and eliminate the false-positive SNPs calls generated by cross hybridization with mouse DNA, we have detected and filtered out reads aligned to mouse reference sequences before doing human whole-exome sequencing analysis; by this way, only specific human calling are considerate. Besides, *KRAS*, *BRAF*, and *PIK3CA* mutations were validated by Sanger method in a different tumor sample.

CGH array analysis

Evaluation of genome-wide, gene copy number was performed using the 250k and 400k oligonucleotide CGH array Agilent technology using two biologic duplicates and two independent experiments. Oligonucleotide array CGH processing was performed as detailed in the manufacturer's protocol (version 6.2 October 2009; http://www.agilent.com). The $\log_2$ ratio and segmentation were generated using Array Studio software. Array Studio, Array Viewer, Array Server, and all other Omicsoft products or service names are registered trademarks or trademarks of Omicsoft Corporation.

Gene expression profiling

The analysis of gene expression was done using U133 Plus Affymetrix microarrays with biologic triplicate (three tumor tissues removed from three distinct mice for each model, passage P6-P9).

Real-time RT-PCR

Affymetrix data of candidate genes were confirmed by qRT-PCR using previously described methodology (9).

Immunohistochemistry

PTEN and INPP4B expression were determined on 4-μm-thick AFA-fixed paraffin-embedded sections. Antigen retrieval was done by incubating tissue sections in an 850-Watt microwave oven for 36 minutes in Tris–EDTA or in citrate buffer for INPP4B and PTEN staining, respectively. Tissue sections were then incubated for 1 hour at room temperature with primary antibodies (anti-INPP4B, clone EPR3108Y, dilution 1:50, rabbit mAb, LSBio; anti-PTEN, clone SP218, dilution 1:50, rabbit mAb, Spring). Staining was revealed by using OmniMap HRP anti-Rabbit (Ventana Medical Systems) and diaminobenzidine (Dako) as chromogen.

Results and Discussion

Comprehensive molecular characterization of tumor samples from colorectal cancer patients has identified a handful of recurrent mutated genes within critical pathways (1, 2, 10). Among these, the PI3K and ERBB–RAS signaling, accurately dissected by the Cancer Genome Atlas Network (TCGA; ref. 2), provide promising therapeutic targets.

To gain more insight into the genomic abnormalities within the PI3K and ERBB–RAS signaling pathways, a large cohort of 52 colorectal PDXs established by the CReMEC consortium (48 MSS and four MSI tumors; ref. 6) was analyzed.

We first examined six genes identified as key upstream elements in the PI3K pathway (2): *IGF2*, *IRS2*, *PIK3CA*, *PIK3R1*, *PTEN*, and *INPP4B* (Fig. 1A, Table 1). Several lines of evidence underline the importance of IGF2 in colorectal cancer. *IGF2* is the single most overexpressed gene in colorectal neoplasia relative to normal colorectal mucosa (11) and loss of imprinting of *IGF2*, one mechanism for its frequent overexpression, is also a risk factor for colorectal cancer (12). More recently, TCGA revealed IGF2 as an important node in the PI3K pathway with mutual exclusion between *IGF2*, *IRS2*, *PIK3CA*, *PIK3R1*, and *PTEN* genomic alterations. Here, gene expression analyses identified *IGF2* overexpression in seven PDXs. As reported in patients (1, 2), *IGF2* overexpression in PDXs (5 out of 7) is mainly due to focal *IGF2* amplification (Fig. 1A and B).

The binding of IGF2 to IGF1R activates the intrinsic tyrosine kinase activity of IGF1R, which results in the phosphorylation of the insulin receptor substrates (IRS), leading to PI3K activation. Gene expression analysis of *IRS1* and *IRS2* revealed no alterations in *IRS1*. However, overexpression of *IRS2* ($n = 5$) was detected in mutually exclusive pattern with *IGF2* amplification or overexpression (Fig. 1A). All *PI3KCA* aberrations ($n = 12$) were oncogenic mutations, affecting all functional domains of the enzyme but with preferential mutation hotspots within exons 9 and 20, as previously described in colorectal cancer (13). *PIK3R1* mutations have been rarely reported in colorectal cancer (2) and none were detected in the present PDX collection.

Two PDXs showed *PTEN* homozygous deletion associated with loss of protein expression, whereas no PTEN mutation was detected (Fig. 1C). Recently, another lipid phosphatase, inositol polyphosphate 4-phosphatase type II (INPP4B), has emerged as a potential tumor suppressor in prostate, breast, and ovarian cancers (14). Downregulation of *INPP4B* gene expression was detected here in two PDXs, with concomitant loss of protein expression. Immunohistochemical analyses confirmed mutual exclusion between PTEN and INPP4B downexpression (Fig. 1C).

Interestingly, a pattern of mutual exclusion in the PI3K pathway also exists between *IGF2*, *IRS2*, *PIK3CA*, *PTEN*, and *INPP4B* alterations. These data imply that therapeutic targeting of the IGF2 pathway could inhibit PI3K activity and suggest *INPP4B* as a tumor suppressor gene in colorectal cancer.

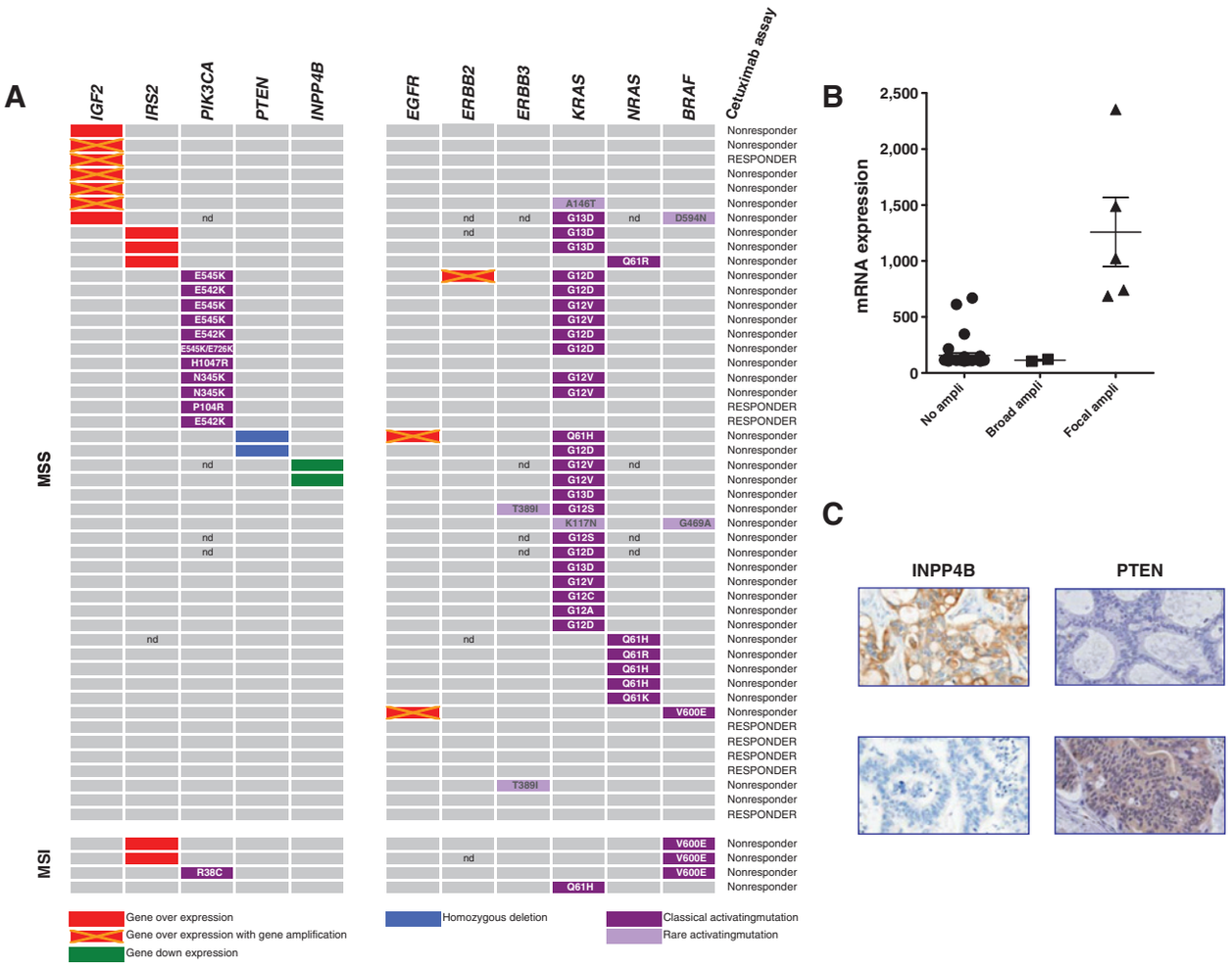

Figure 1.
Molecular alterations of the IGF2–PI3K and ERBB–RAS pathways in MSS and MSI colorectal cancer xenografts. A, genomic alterations of the IGF2–PI3K and ERBB–RAS pathways. Mutations were determined by NGS. Tumors were considered to be amplified if the gene copy number was >3 using CGH array analysis. Gene overexpression is defined by an expression superior to average in all PDX panel + 1 SD. B, correlation of expression levels with copy-number changes for *IGF2*. Amplification, >3 gene copy; focal amplification, <10 genes. C, *in situ* expression of PTEN and INPP4B proteins. Anti-PTEN and INPP4B immunohistochemistry results for representative negative (blue staining) and positive (brown staining) PDXs. Magnification, ×40.

Mutations or gene amplification of candidate genes in the ERBB–RAS pathway was then analyzed. *EGFR* displayed no mutations but gene amplification associated with gene overexpression in two MSS PDXs. No mutation was identified in *ERBB2*, but one PDX showed *ERBB2* amplification, accompanied by overexpression. Two PDXs displayed a T389I *ERBB3* mutation, probably damaging (PolyPhen prediction software). No gene alteration was present in *ERBB4*.

We found that 69% (33 of 48) of MSS tumors and 100% (4 of 4) of MSI tumors have oncogenic alterations in *KRAS*, *NRAS*, or *BRAF* with a significant pattern of mutual exclusion (Fig. 1A). In accordance with published data, *KRAS* missense mutations in codons 12, 13, and 61 were the most frequent *KRAS* mutations (observed mutated in 18, 5 and two PDX models, respectively). Two additional PDXs showed two oncogenic *KRAS* mutations, K117N and A146T, previously reported in colorectal cancer with similar low frequencies (1, 15). Six PDXs displayed *NRAS* mutations, with all mutations occurring in codon 61. Six PDXs displayed *BRAF* mutations: four of these were the frequent hot-spot V600E mutation and two were less frequent mutations, D594N and G469A, already reported in colorectal cancer (16). *BRAF* V600E mutations were associated with MSI, as this mutation was present in 75% (3 of 4) of MSI tumors compared with 2% (1 of 48) of MSS tumors, ($P < 0.0001$, Yates χ^2 test). *BRAF* V600E mutations were mutually exclusive from *KRAS* and *NRAS* mutations as usually described (16).

Finally, we observed no significant association of alterations in the RAS and PI3K pathways, suggesting that simultaneous inhibition of the RAS and PI3K pathways might be necessary for successful therapy in the subgroup displaying cooccurrence of these molecular alterations.

These genomic analyses enable an assessment of the diversity and the frequency of genomic changes altering these two major signaling pathways in our colorectal cancer PDX models and

Table 1. The 52 PDXs have been analyzed for gene expression and gene copy number

	Patient tumor information				Gene expression												Gene copy number			
					IGF2			IRS2		EGFR		ERBB2		INPP4B						
	Tumor site	Primary tumor location	Stage	Microsat status	qRT-PCR	202409_at	210881_s_at	qRT-PCR	209184_s_at	qRT-PCR	201983_s_at	qRT-PCR	216836_s_at	qRT-PCR	205376_at	IGF2	EGFR	ERBB2	INPP4B
PDX #1	Primary	Left	pT3N0M0	MSS	3	76	136	1268	1033	495	1424	1646	1684	1268	468	2.51	2.51	2.58	1.84
PDX #2	Primary	Rectum	pT4N1M0	MSS	2	67	114	1589	948	273	1075	853	1236	30	164	1.82	2.75	2.32	1.68
PDX #3	Metastasis	Left	pT4N1M1	MSS	31538	5790	348	2431	1083	488	695	2186	1184	55	29	2.15	2.27	2.41	1.21
PDX #4	Primary	Left	pT2N0M0	MSS	11	65	119	5972	3682	513	1550	1622	1054	506	332	2.44	2.79	2.27	2.05
PDX #5	Metastasis	Right	pT3N2M1	MSS	1	69	114	1256	1141	451	947	1621	1811	451	259	2.36	2.46	3	1.85
PDX #6	Metastasis	Left	pT2N1M1	MSS	384	67	123	1117	833	1037	1561	1158	1275	236	218	2.17	5.09	2.2	1.48
PDX #7	Primary	Right	pT3N1M1	MSS	3124	10989	669	637	438	42	69	386	585	192	172	2.44	2.32	1.75	2.13
PDX #8	Metastasis	Right	pT3N1M1	MSS	102	69	125	970	764	229	910	1279	703	424	135	1.61	3.03	1.63	2.09
PDX #9	Primary	Left	pT3N0M0	MSS	4	71	150	4526	1848	617	598	1951	846	531	70	2.36	2.7	1.47	1.34
PDX #10	Metastasis	Right	pT2N1M1	MSS	ND	17017	612	2289	1918	444	778	1465	1581	563	110	2.09	1.86	1.94	1.81
PDX #11	Metastasis	Left	pT4N0M0	MSS	20	839	137	571	1035	256	786	2198	2100	489	247	2.14	2.55	3.96	1.3
PDX #12	Primary	Right	pT3N0M0	MSS	44	59	117	4263	2927	762	1189	2401	1713	689	542	2.5	3.77	2.36	2.16
PDX #13	Primary	Left	pT3N1M1	MSS	6	198	122	589	614	455	1127	927	1261	221	47	3.03	2.04	1.46	2.19
PDX #14	Metastasis	Left	pT3N1M1	MSS	7	61	116	1303	777	859	1233	1187	1190	440	162	2.65	3.51	1.95	2.09
PDX #15	Primary	Rectum	pT2N0M0	MSS	453217	29902	2354	431	546	303	826	1081	1292	255	190	5	2.44	2.49	1.84
PDX #16	Metastasis	Left	pT3N0M1	MSS	3	76	125	6939	1920	1013	1098	2070	975	1504	159	2.98	3.33	1.9	1.71
PDX #17	Metastasis	Left	pT4N1M1	MSS	47	230	122	17254	4728	416	783	1934	1242	423	253	2.02	2.01	2.11	1.96
PDX #18	Primary	Left	pT4N1M1	MSS	26	64	124	5582	2774	167	536	818	1413	179	162	2.07	2.16	2.15	1.49
PDX #19	Primary	Left	pT2N1M0	MSS	128707	21436	687	789	410	296	577	2429	1885	1564	285	3.38	2.49	2.57	1.86
PDX #20	Primary	Left	pT3N1M1	MSS	3	97	117	5793	3261	374	1085	1025	1565	1347	501	2.13	2.12	1.51	1.42
PDX #21	Primary	Rectum	pT4N0M0	MSS	3	66	106	2056	1091	984	1345	2004	1442	1424	447	3.4	2.65	2.35	1.55
PDX #22	Primary	Rectum	pT3N2M1	MSS	27	86	138	6353	3169	241	767	1008	1165	456	252	2.16	2.59	1.99	1.32
PDX #23	Primary	Right	pT3N1M0	MSS	8	65	114	7049	1531	1185	1219	3538	1570	4545	372	1.85	2.25	1.62	2.17
PDX #24	Primary	Left	pT3N2M1	MSS	51	81	120	3164	1647	400	787	1269	977	827	410	2.08	2.05	2.15	2.03
PDX #25	Carcinosis	Left	pT4N0M0	MSS	15	55	106	930	578	462	774	2848	1623	865	158	1.79	1.77	2.62	1.76
PDX #26	Primary	Rectum	pT3N2M0	MSS	107	64	128	1852	2284	341	833	3302	1359	594	216	2.23	1.98	2.95	1.96
PDX #27	Primary	Rectum	pT3N2M0	MSS	3	72	114	8003	2179	206	489	2681	1293	819	207	1.96	1.95	1.99	1.94
PDX #28	Primary	Left	pT3N1M1	MSS	39	86	120	112	1339	453	885	8657	2888	965	224	2.14	2.44	9.67	1.21
PDX #29	Metastasis	Right	pT3N0M1	MSS	3	83	105	1311	249	568	823	1071	5896	574	394	2.47	4.31	1.54	1.49
PDX #30	Primary	Rectum	pT3N2M0	MSS	0	68	126	3576	672	241	1534	1181	903	619	232	2.27	2.06	2.09	1.4
PDX #31	Primary	Right	pT3N0M1	MSS	0	69	118	735	732	416	1151	1766	2138	852	188	1.38	2.15	2.25	1.13
PDX #32	Primary	Left	pT3N2M1	MSS	9	82	127	208	393	434	1259	1691	1936	885	207	1.68	2.83	2.17	1.48
PDX #33	Primary	Right	pT3N2M1	MSS	16573	3521	216	5779	2368	1606	2423	1767	1302	852	419	2.46	3.63	2.38	1.3
PDX #34	Carcinosis	Right	pT4N2M1	MSS	3	56	115	2026	1612	700	1562	1528	1592	741	272	1.72	2.23	1.56	1.52
PDX #35	Primary	Rectum	pT3N2M0	MSS	0	68	143	2708	1645	566	1074	761	955	44	30	1.29	2.17	2.28	1.12
PDX #36	Primary	Left	pT3N1M1	MSS	109409	26618	1489	1469	2033	249	1052	724	1374	171	162	4.05	2.51	2.62	1.87
PDX #37	Metastasis	Left	pT3N1M1	MSS	117346	22391	741	1558	1678	219	723	585	937	434	285	4.16	2.66	1.63	2.15
PDX #38	Metastasis	Left	pT3N1M1	MSS	154	92	106	3975	2706	528	1364	1684	1841	1100	618	1.95	2.39	2.41	1.63
PDX #39	Primary	Right	pT3N0M0	MSS	137361	23511	1023	990	501	339	989	1133	1344	711	223	3.26	2.01	2.1	1.5
PDX #40	Metastasis	Left	pT4NxM1	MSS	20	93	123	1968	1107	425	895	1617	1273	872	284	ND	ND	ND	1.93
PDX #41	Carcinosis	Left	pT4NxM1	MSS	1688	68	122	4003	2175	490	888	2176	1139	1531	326	2	1.98	2.02	1.95
PDX #42	Primary	Right	pT4N2M1	MSS	4	72	123	900	642	186	347	1843	1720	636	165	2.98	2.57	3.33	1.18
PDX #43	Metastasis	Right	pT4N2M1	MSS	2	66	112	1462	1015	175	349	1457	1526	809	195	2.33	2.4	2.44	1.21
PDX #44	Carcinosis	Left	NA	MSS	3	69	121	5976	2530	696	1122	2348	1771	656	203	2.31	3.09	2.66	1.24
PDX #45	Primary	Left	pT3N1M0	MSS	369	ND	ND	6989	ND	726	ND	1607	ND	2741	ND	2.5	2.2	2.63	1.78
PDX #46	Primary	Right	pT3N1M1	MSS	1	76	129	1775	1412	409	896	929	1061	375	209	1.93	2.49	1.79	1.68
PDX #47	Primary	Left	pT3N1M0	MSS	22	76	133	5343	1820	663	1072	1301	892	736	168	2.47	2.48	1.37	1.28
PDX #48	Carcinosis	Left	pT3N1M1	MSS	2	ND	ND	5567	ND	307	ND	973	ND	773	ND	2.64	2.23	1.61	1.48
PDX #49	Primary	Right	pT4N0M0	MSI	0	ND	ND	7060	ND	546	ND	2742	ND	458	ND	2	1.98	2.04	1.97
PDX #50	Primary	Right	pT4N1M0	MSI	0	67	135	6806	3154	458	606	2335	2051	513	139	1.97	1.96	1.99	1.95
PDX #51	Primary	Left	pT4N1Mx	MSI	11	75	125	4174	1724	749	1485	2005	1731	326	113	2.02	2.31	2.6	1.48
PDX #52	Primary	Right	pT3N0M0	MSI	504	152	135	1792	861	472	92	839	908	829	156	1.97	1.96	2.01	1.95

NOTE: Gene expression value measured by qRT-PCR is expressed as normalized expression. For each gene, only probe sets specific for gene transcript sequences have been analyzed.

Abbreviation: NA, not applicable.

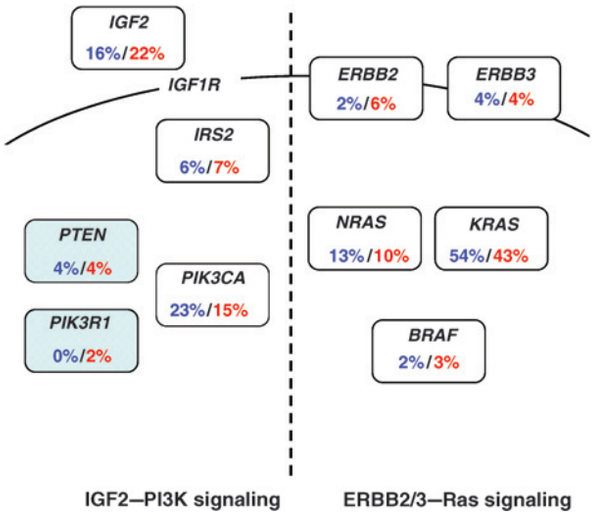

Figure 2.
Diversity and frequency of genetic changes leading to deregulation of IGF2–PI3K and ERBB–RAS signaling pathways in the colorectal cancer patient-derived xenograft panel compared with published human tumors. MSS xenografts were analyzed for somatic mutations (*ERBB2*, *ERBB3*, *KRAS*, *NRAS*, *BRAF* V600E, *PIK3CA*, *PIK3R1*), homozygous deletion (*PTEN*), amplifications (*IGF2*, *ERBB2*), and significant gene overexpression (*IGF2*, *IRS2*). Alteration frequencies are expressed as a percentage of the 50 MSS xenografts in blue. Data obtained in nonhypermutated patient tumor samples reported by TCGA (2) are noted in red.

comparison with TCGA data (Fig. 2). TCGA has reported that 77% (23 of 30) of hypermutated tumors are MSI tumors (2). As the present PDX collection displays a low frequency of MSI tumors (4 of 52, 8%) close to that of patient tumors (23 of 224, 10%; ref. 2), we focused on MSS PDX and patient tumors. The frequency of studied molecular epidemiology data from these two groups showed remarkable concurrence, suggesting that the PDX bank represents a useful set of preclinical models for testing new therapies and emphasizing the potential therapeutic value of targeting IGF2 in colorectal cancer. In the same way, recent analyses by the Bodmer laboratory have shown that *in vitro* colorectal cancer cell lines provide useful preclinical tools because of well represented genetic diversity of patient tumors in cell lines (17, 18). It led us to an analysis of gene abnormalities specifically within IGF2–PI3K pathway in a large panel of 62 human colorectal cancer cell lines using the Broad–Novartis Cancer Cell Line Encyclopedia data (http://www.broadinstitute.org/ccle/home). We carefully separated MSS and MSI cell lines because of overpresentation of MSI cell lines, which could interfere with mutation frequencies. IGF2–PI3K pathway alterations appear almost mutually exclusive within the 36 MSS cell lines with some redundancy between *PIK3CA* activating mutations and *IRS2* overexpression (Supplementary Fig. S1). Whereas *PIK3CA*, *PTEN*, and *PIK3R1* aberration profiles recapitulate the patient tumor observation, the frequencies of *IGF2* and *IRS2* upregulation in MSS colorectal cancer cell lines are under- and overrepresented, respectively.

In addition to maintaining the genomic and histologic heterogeneity, translationally relevant preclinical models need to reproduce drug response observed in patients. Although *KRAS* mutations had been identified as a strong predictive biomarker of resistance to cetuximab and panitumumab (3), only a subset of *KRAS* wild-type (WT) patients respond to anti-EGFR MAbs, underlining that additional predictive biomarkers exist within *KRAS* WT tumors. The characterization of alterations occurring in additional candidate genes (*NRAS*, *BRAF*, *PIK3CA*, *PTEN*) increased indeed the negative predictive value up to 70%, but it is not sufficient to identify all resistant cases (19).

To assess drug response prediction in our PDX models, cetuximab response was analyzed in the PDX panel. To be consistent with clinical criteria, we considered responders the PDXs displaying partial or complete response and nonresponders the PDXs displaying growth stabilization or progression (Supplementary Fig. S2). With these scoring criteria, eight out of 52 PDXs (15%) were responders to cetuximab, with complete tumor disappearance in three PDX models. The all eight responders were WT *KRAS* tumors (Figs. 1A and 3), outlining the requirement of WT *KRAS* genotype for clinical benefit. This low proportion of PDX responders in an unselected population (15%) is highly concordant with patient data (8) and PDX data from an independent metastatic colorectal cancer xenograft series (7). Noteworthy, cetuximab has been shown to be active against *KRAS*-mutated xenografts (6), leading to a statistically significant reduced tumor growth but with no tumor shrinkage. This kind of PDX response means nevertheless progressive disease from a clinical point of view. Therefore, assessment parameters have to be carefully analyzed to avoid over- or misinterpretation of drug efficacy.

The majority of nonresponder PDXs (27 of 44) showed canonical activating mutations in *KRAS* (codons 12, 13, 61, 117, and 146). The Trusolino group reported similar results involving *KRAS* mutations in codons 61, 117, and 146 in primary resistance to cetuximab in a large and independent colorectal PDX series (7). While most clinical studies limited *KRAS* mutation assessment to codons 12–13, *KRAS* codon 61 and 146 mutations, in addition to *NRAS* and *BRAF* mutations, have also been shown in retrospective studies to predict resistance to cetuximab or panitumumab in WT *KRAS* codon 12 and 13 metastatic colorectal cancer (19, 20). The European Medicines Agency recently updates and restricts the indication for cetuximab to WT *RAS* metastatic colorectal cancer (not only WT *KRAS* codon 12–13).

Likewise, none of the four *BRAF* V600E–mutated, four *NRAS*-mutated, and four *KRAS* (codon 61, 117 or 146) mutated PDXs responded to cetuximab with tumor shrinkage. Therefore, exclusion of these mutations enables an improved selection of PDXs likely to respond to cetuximab, increasing the response rate from 28% (8 out of 29 12–13 codons *KRAS* WT) to 53% (8 of 15) in PDXs that are fully wild-type for all three genes, as reported retrospectively in patients (19, 20). This study functionally cross validates a recent clinical stratification based on combination of predictive biomarkers obtained retrospectively in patients (19). These data support the utility of our PDX panel for identifying predictors of drug response in metastatic colorectal cancer patients.

As for *PTEN* and *PIK3CA* impact, clinical data are more conflicting (8, 13, 19). In the present preclinical work, only *PTEN* homozygous deletion, leading to absolute *PTEN* inactivation, has been taken into account. This *PTEN* loss occurred within *KRAS*-mutated xenografts, displaying lack of response to cetuximab. Individual contribution of *PIK3CA* mutations to the

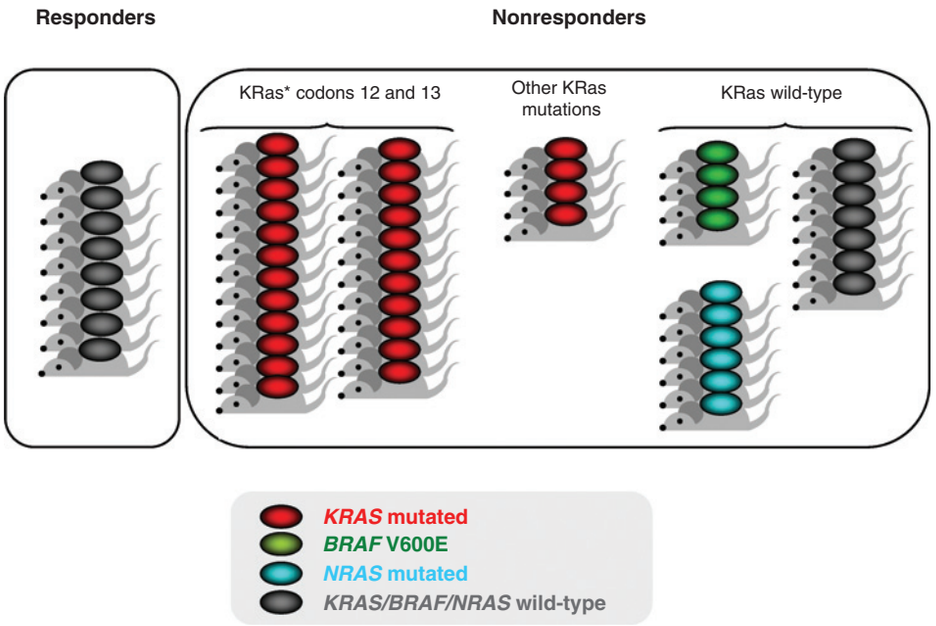

Figure 3.
Graphic representation of the cohort of 52 colorectal xenografts treated with cetuximab. Molecular alterations mutually exclusive or coexisting are indicated according to different color codes.

absence of response is difficult to assess because of the *PIK3CA* mutation diversity in different protein domains and coexistence of these mutations with *KRAS* and *BRAF* mutations (13). Moreover, one PDX with *IGF2* activation and two other PDXs with *PIK3CA* mutation respond to cetuximab. Among the five IGF2-overexpressed KRAS WT tumors, only one responds to cetuximab. Taken together, these data suggest that IGF2–PI3K components are not biomarkers of resistance to anti-EGFR therapies and underline the interest to combine anti-IGF2 and anti-EGFR treatment.

Within the group of 15 *KRAS/BRAF/NRAS* wild-type PDXs, further investigation has been performed for additional putative predictive biomarkers of resistance to anti-EGFR (8, 21): *EGFR* gene amplification, overexpression and mutation; gene overexpression of two EGFR ligands (epiregulin and amphiregulin), *MET* gene amplification and overexpression, *KRAS* gene amplification and *HRAS* mutation (Supplementary Table S1). Noteworthy, none of the patients with colorectal cancer, from whom the triple wild-type PDXs were derived, had been exposed to anti-EGFR therapy before surgery, ruling out the possibility of acquired resistance in the pretreated PDXs. The analysis of these parameters did not allow to statistically discriminating between the responder and nonresponder groups (Fisher exact test, $P > 0.05$). Nevertheless, it is noteworthy that cetuximab treatment was ineffective in mice engrafted with the three PDX models carrying *KRAS* amplification.

Collectively, the present data demonstrate the relevance of colorectal PDXs as models for preclinical drug development. The PDX models remarkably fit the molecular epidemiology and the cetuximab drug response profiles of colorectal cancer patient populations, justifying the growing use of mouse clinical trials in cancer drug development and decision making (5). More importantly, these data support the identification of *KRAS* (exon 2, 3, and 4)/*NRAS*/*BRAF* wild-type patients for treatment with cetuximab, and IGF2 as an attractive novel cancer drug target in a large subset of colorectal cancer patients.

Disclosure of Potential Conflicts of Interest

P. Vrignaud is an employee of and is a stock holder of Sanofi. J. Watters is Head, Translational Medicine Oncology, at Sanofi. No potential conflicts of interest were disclosed by the other authors.

Authors' Contributions

Conception and design: M. Nunes, I. Bièche, V. Dangles-Marie
Development of methodology: M. Nunes, S. Vacher, S. Richon, C. Dib, I. Bièche
Acquisition of data (provided animals, acquired and managed patients, provided facilities, etc.): P. Vrignaud, S. Vacher, S. Richon, W. Cacheux, L.-B. Weiswald, S. Chateau-Joubert, C. Dib, J. Watters, I. Bièche
Analysis and interpretation of data (e.g., statistical analysis, biostatistics, computational analysis): M. Nunes, P. Vrignaud, S. Vacher, A. Lièvre, W. Cacheux, G. Massonnet, S. Chateau-Joubert, W. Zhang, D. Bergstrom, I. Bièche, V. Dangles-Marie
Writing, review, and/or revision of the manuscript: M. Nunes, P. Vrignaud, S. Richon, A. Lièvre, W. Cacheux, L.-B. Weiswald, J. Watters, D. Bergstrom, S. Roman-Roman, I. Bièche, V. Dangles-Marie
Administrative, technical, or material support (i.e., reporting or organizing data, constructing databases): A. Nicolas, V. Dangles-Marie
Study supervision: M. Nunes, P. Vrignaud, V. Dangles-Marie

Acknowledgments

We thank CReMEC consortium and especially Ludovic Lacroix, Ludovic Bigot, Fariba Nemati, Cyril Berthet and Olivier Duchamp for PDX tissues and nucleic acid managing and valuable discussions. Additional acknowledgments go to all the additional scientific collaborators from the "Institut Curie Digestive Group" led by Sylvie Robine. We thank Didier Meseure and Jean-Jacques Fontaine for help in histological analyses.

Grant Support

This work was supported by the Comité départemental des Hauts-de-Seine de la Ligue Nationale Contre le Cancer, the Conseil régional d'Ile-de-France, and the Cancéropôle Ile-de-France and the Association pour la recherche en cancérologie de Saint-Cloud (ARCS), Genevieve and Jean-Paul Driot Transformative Research Grant, Philippe and Laurent Bloch Cancer Research Grant, Hassan Hachem Translational Medicine Grant, and Sally Paget-Brown Translational Research Grant.

Received May 28, 2014; revised September 17, 2014; accepted February 6, 2015; published OnlineFirst February 24, 2015.

References

1. Seshagiri S, Stawiski EW, Durinck S, Modrusan Z, Storm EE, Conboy CB, et al. Recurrent R-spondin fusions in colon cancer. Nature 2012;488:660–4.
2. Network TCGA. Comprehensive molecular characterization of human colon and rectal cancer. Nature 2012;487:330–7.
3. Lievre A, Blons H, Laurent-Puig P. Oncogenic mutations as predictive factors in colorectal cancer. Oncogene 2010;29:3033–43.
4. Dangles-Marie V, Pocard M, Richon S, Weiswald LB, Assayag F, Saulnier P, et al. Establishment of human colon cancer cell lines from fresh tumors versus xenografts: comparison of success rate and cell line features. Cancer Res 2007;67:398–407.
5. Tentler JJ, Tan AC, Weekes CD, Jimeno A, Leong S, Pitts TM, et al. Patient-derived tumour xenografts as models for oncology drug development. Nat Rev Clin Oncol 2012;9:338–50.
6. Julien S, Merino-Trigo A, Lacroix L, Pocard M, Goere D, Mariani P, et al. Characterization of a large panel of patient-derived tumor xenografts representing the clinical heterogeneity of human colorectal cancer. Clin Cancer Res 2012;18:5314–28.
7. Bertotti A, Migliardi G, Galimi F, Sassi F, Torti D, Isella C, et al. A molecularly annotated platform of patient-derived xenografts ("xenopatients") identifies HER2 as an effective therapeutic target in cetuximab-resistant colorectal cancer. Cancer Discov 2012;1:508–23.
8. Bardelli A, Siena S. Molecular mechanisms of resistance to cetuximab and panitumumab in colorectal cancer. J Clin Oncol 2010;28:1254–61.
9. Bieche I, Parfait B, Le Doussal V, Olivi M, Rio MC, Lidereau R, et al. Identification of CGA as a novel estrogen receptor-responsive gene in breast cancer: an outstanding candidate marker to predict the response to endocrine therapy. Cancer Res 2001;61:1652–8.
10. Wood LD, Parsons DW, Jones S, Lin J, Sjoblom T, Leary RJ, et al. The genomic landscapes of human breast and colorectal cancers. Science 2007;318:1108–13.
11. Zhang L, Zhou W, Velculescu VE, Kern SE, Hruban RH, Hamilton SR, et al. Gene expression profiles in normal and cancer cells. Science 1997;276:1268–72.
12. Cui H, Cruz-Correa M, Giardiello FM, Hutcheon DF, Kafonek DR, Brandenburg S, et al. Loss of IGF2 imprinting: a potential marker of colorectal cancer risk. Science 2003;299:1753–5.
13. Perrone F, Lampis A, Orsenigo M, Di Bartolomeo M, Gevorgyan A, Losa M, et al. PI3KCA/PTEN deregulation contributes to impaired responses to cetuximab in metastatic colorectal cancer patients. Ann Oncol 2009;20:84–90.
14. Agoulnik IU, Hodgson MC, Bowden WA, Ittmann MM. INPP4B: the new kid on the PI3K block. Oncotarget 2011;2:321–8.
15. Wojcik P, Kulig J, Okon K, Zazula M, Mozdzioch I, Niepsuj A, et al. KRAS mutation profile in colorectal carcinoma and novel mutation–internal tandem duplication in KRAS. Pol J Pathol 2008;59:93–6.
16. Samowitz WS, Sweeney C, Herrick J, Albertsen H, Levin TR, Murtaugh MA, et al. Poor survival associated with the BRAF V600E mutation in microsatellite-stable colon cancers. Cancer Res 2005;65:6063–9.
17. Mouradov D, Sloggett C, Jorissen RN, Love CG, Li S, Burgess AW, et al. Colorectal cancer cell lines are representative models of the main molecular subtypes of primary cancer. Cancer Res 2014;74:3238–47.
18. Wilding JL, Bodmer WF. Cancer cell lines for drug discovery and development. Cancer Res 2014;74:1–8.
19. De Roock W, Claes B, Bernasconi D, De Schutter J, Biesmans B, Fountzilas G, et al. Effects of KRAS, BRAF, NRAS, and PIK3CA mutations on the efficacy of cetuximab plus chemotherapy in chemotherapy-refractory metastatic colorectal cancer: a retrospective consortium analysis. Lancet Oncol 2012;11:753–62.
20. Oliner KS, Douillard JY, Siena S, Tabernero J, Burkes RL, Barugel ME, et al. Analysis of KRAS/NRAS and BRAF mutations in the phase III PRIME study of panitumumab (pmab) plus FOLFOX versus FOLFOX as first-line treatment (tx) for metastatic colorectal cancer (mCRC). J Clin Oncol 2013;31:abstract 3511.
21. Leto SM, Trusolino L. Primary and acquired resistance to EGFR-targeted therapies in colorectal cancer: impact on future treatment strategies. J Mol Med 2014;92:709-.